PPPL-2208 130 5-24-85 85 ① DR-1020-0 PPPL-2208

UC20-A

I-21084

ION CYCLOTRON HEATING EXPERIMENTS IN PLT

By

E. Mazzucato *et al.*

MASTER

MARCH 1985

PLASMA PHYSICS LABORATORY

PRINCETON UNIVERSITY
PRINCETON, NEW JERSEY

PREPARED FOR THE U.S. DEPARTMENT OF ENERGY,
UNDER CONTRACT DE-AC02-76-CHO-3073.

PPPL--2208
DE85 011690

ION CYCLOTRON HEATING EXPERIMENTS IN PLT

E. Mazzucato, R. Bell, M. Bitter, A. Cavallo, S. Cohen,
P. Colestock, G. Greene, G. Hammett, E. Hinnov, J. Hosea,
D. Hwang, R. Kaita, S. Lippmann, J. Lovberg, D. McNeill, D. Mueller
M. Ono, C.K. Phillips, G. Schilling, C. Skinner
S. Suckewer, and J.R. Wilson

Plasma Physics Laboratory, Princeton, New Jersey 531 3000
P.O. Box 451, Princeton, NJ 08544

ABSTRACT

Results from ICRF heating experiments in the D-^{3}He minority regime on the PLT tokamak are reported. At the highest coupled rf power of 2.6 MW, a central ion temperature of 3.6 keV has been measured in plasmas with a central density of $5 \times 10^{13} cm^{-3}$. The central value of the electron temperature is strongly modulated by the sawtooth internal relaxation and reaches values in excess of 3 keV. No deterioration of the ion heating efficiency has been found in the investigated range of plasma parameters.

I. INTRODUCTION

The PLT research program on plasma heating in the Ion Cyclotron Range of Frequencies (ICRF) is directed toward the demonstration that this is a viable method for heating a reactor to ignition. To achieve this goal PLT operation must be extended to plasma conditions as close as possible to those contemplated for larger devices.

Very promising results obtained on PLT in both the minority fundamental and the majority second harmonic heating regimes have been reported previously [1,2]. Since the best heating efficiency has been found for the ^{3}He minority regime, we have converted all three of the existing sources to 30 MHz so that we can explore this regime at a power level of up to ~ 5 MW with a relatively high toroidal field of ~ 30 kG. In this paper we present the first results obtained on PLT with the new ICRF system at a power level of up to 2.6 MW coupled to the plasma.

II. PLT ICRF SYSTEM

In previous experiments, the power limit per one half-turn loop antenna on PLT was approximately 0.5 MW. This power capability is far below the power density requirement for future high density heating experiments. A redesign of the rf vacuum feedthrough has permitted a substantial increase in the individual antenna and overall power handling capability [3]. Presently, all PLT antennas are fed with the new feedthroughs, with a maximum power of 1.5 MW delivered to a single half-turn antenna.

The experimental results presented in this paper were obtained with three half-turn antennas on the low field side of the torus, and a maximum power of ~ 3 MW at 30 MHz. Two of these antennas are located in adjacent ports (45 cm apart) and are phased 180° with respect to each other, thus giving an $n_\parallel$ spectrum peaked at ~ 10. The third antenna is ~ 135 cm from the first pair and imposes a broad $n_\parallel$ spectrum centered about 0. Of the 3 MW delivered to the three antennas, approximately 85%, or 2.6 MW, is coupled to the PLT plasma.

III. EXPERIMENTAL RESULTS

In the ICRF experiments described in this paper, ^{3}He has been used as the minority species in a deuterium plasma with the toroidal magnetic field in the range of 30-32 kG. The main limiters were top-bottom carbon mushrooms located toroidally 90 cm away from the nearest antenna. An auxiliary limiter was located in the midplane on the outside of the torus.

Previous studies have shown that the plasma current in PLT must be maintained at values above 300 kA to prevent a precipitous drop in the ion heating efficiency and the simultaneous influx of impurities [4]. For this reason the plasma current was maintained in the range of 500-600 kA.

Typical parameters of the target ohmic plasma were a central electron temperature T_{eo} ~ 1.5 keV, a central ion temperature T_{io} ~ 1 keV, and a line average density $\bar{n}_e$ ~ 2-4 x 10^{13}cm^{-3}. The value of Z_{eff} derived from the measured electron temperature and density profiles was in the range 1-1.5.

One characteristic feature of ICRF in PLT is a density increase during the rf pulse. This is shown in Fig. 1 where the time evolution of $\bar{n}_e$ is shown for 2.6 MW of rf power into the plasma. We found that the density increase tends to saturate with rf power. We also found that the density during the ICRF pulse depends very weakly on the target plasma density so that low density discharges are strongly perturbed by the rf and, therefore, are more difficult to control at large power levels.

An increase in the charge-exchange outflux of low energy (< 1 keV) neutrals was observed during the ICRF heating pulse. This flux is apparently toroidally uniform and was measured to be linearly dependent on ICRF power, and about equal to 10^{15} cm^{-2} s^{-1} MW^{-1} [5]. An increase in the H_α emission was also measured at several locations around the torus. These observations suggest that the density increase caused by ICRF is predominately due to an increase in recycling at the vacuum vessel wall, although a small fraction of the density increase is due to an influx of impurities (see below). We have also found that the charge-exchange outflux increases significantly for plasma currents below ~ 300 kA. This current threshold effect parallels that for impurity influx, and suggests that fast ion losses may trigger the increase in recycling.

Minority concentrations, $\eta = n_{^3He}/n_e$, of 10% or smaller were used in the ICRF experiments. The density of ^{3}He was estimated from the increase of $\bar{n}_e$ produced by the injection of ^{3}He into the discharge. Our study of the mode conversion of fast magnetosonic waves into ion Bernstein waves indicates that this is a good estimate of the ^{3}He concentration in the central part of the plasma torus [4]. In this study, density fluctuations at the ICRF frequency were detected with the scattering of microwaves at a fixed position on the midplane. The magnetic field necessary to localize an ion Bernstein wave with a well defined wave vector inside the scattering region was measured. The measurements at several values of the wave vector were then fitted to the kinetic dispersion relation. The only free parameter was the minority concentration. The values obtained for η agree (within $\pm$ 20%) with those estimated from the changes of $\bar{n}_e$ induced by the puffing of ^3He.

Three techniques have been used for determining the ion temperature: charge-exchange measurements, Doppler broadening of impurity line radiation, and neutron emission measurements. This redundancy is necessary because each method has intrinsic uncertainties. Together these measurements provide a consistent picture of the ion heating.

In order to determine the central deuterium ion temperature, T_d, from charge-exchange measurements, the measured value, T_{cx}, must be corrected to account for the effects of radial profiles of the plasma parameters on the energy distribution of escaping neutrals. The neutral density profile, which is not directly measured, is calculated assuming an edge neutral density and temperature. The time evolution of T_d derived from charge-exchange measurements is shown in Fig. 2 for a discharge with $\bar{n}_e = 3.8 \times 10^{13}$ cm^{-3} and 2.6 MW of coupled rf power. For this case the calculated correction factor is 1.1.

The second method used for determining the ion temperature is Doppler broadening of impurities lines, FeXXV (for T_d in the center), FeXX (for T_d at $r \sim 20$ cm). and CV and CIII (for T_d at the edge). While this method can provide a precise measurement of the impurity ion temperature, T_{imp}, it suffers from the fact that the value of T_{imp} may be different from that of T_d. In fact, since both deuterium and impurity ions are heated by collisions with the ^3He *hot component*, the power per ion scales approximately like Z_i^2/m_i. We can estimate a lower limit of the ratio T_d/T_{imp} by assuming that the only loss of energy suffered by the impurity ions, which may all be assumed to have the same temperature, owing to their strong coupling, is due to collisions with the background deuterium. The power deposition to the ions is estimated using the value of the central power deposition to the electrons, which is derived from the time evolution of the electron temperature (see below), and a calculation of the ^3He energy distribution using an isotropic quasilinear rf diffusion model, which has shown good agreement with the observations in the case of D-H minority heating [6]. The resultant temperature difference which can be supported by the collisional coupling between impurities and deuterons is estimated to be ~ 400 eV for the highest measured T_{imp} ~ 4 keV. The corrected values of T_d derived from FeXXV Doppler broadening measurements are shown in Fig. 2 for the 2.6 MW case.

Finally, the central values of T_d are obtained from neutron flux measurements, taking into account the deuterium depletion due to impurities. By using the plasma composition derived from spectroscopic measurements (Fig. 3), we obtain the values of T_d shown in Fig. 2 for the 2.6 MW case.

The spectroscopic results of Fig. 3 reveal not only that most of the deuterium depletion is caused by oxygen and carbon impurities (in addition to that attributable to ^3He), but that the bulk of the radiation (Fig. 1) is caused by these lighter impurities in the periphery of the plasma. The higher

Z impurities give a radiation contribution from the central region of ~ 0.2 - 0.3 W cm^{-3} and contribute somewhat to the value of Z_{eff} which almost doubles during the rf pulse for the case shown.

Figure 4 shows the radial profiles of T_d derived from Doppler broadening measurements for several values of rf power and $\bar{n}_e \simeq 3.8 \times 10^{13}$ cm^{-3}. Figure 5 shows the dependence of the ion temperature increase on rf power and plasma density. These data indicate that, within the range of rf power and density investigated, the ion heating efficiency remains approximately constant.

The electron temperature, T_e, was obtained from the measure of the plasma emission at the second harmonic of the electron cyclotron frequency and from Thomson scattering of laser light. Figure 6 shows the time evolution of T_e at four radial locations for the 2.6 MW case. The central value of T_e is strongly modulated by the sawtooth relaxation. The same phenomenon is seen in Fig. 7 which shows the radial profiles of T_e at the top of a sawtooth and 1 msec after the internal disruption. Another effect produced by large rf powers is the flattening of the central part ($r < 20$ cm) of the density profile.

Figure 8 contains the time evolution of the central value of T_e during a sawtooth period. These data show that the slope of T_e at the beginning of the sawtooth steadily increases with power, but neither the amplitude nor the period of the oscillation are strong functions of rf power at large power levels. Figure 9 shows the quantity $p_e = 1.5\, n_e(o)dT_e(o)/dt$ at the beginning of a sawtooth oscillation as a function of rf power for a constant value of n ~ 0.07. If we neglect the electron thermal losses in the center of the discharge over the first part of the sawtooth period, p_e is a measure of the central power deposition to the electrons. These data indicate that p_e increases with rf power and has a value of ~ 1 W cm^{-3} at 2 MW. We have also found that the value of p_e is a growing function of η (Fig. 9). This must be considered a clear indication that other processes (i.e., mode conversion), besides collisions with the hot minority component, play a role in the ICRF heating.

IV. DISCUSSION

The results of Figs. 4 and 5 indicate that no catastrophic ion energy loss has been encountered as the ICRF power to the antennas was raised to the 3 MW level. This is also shown in Fig. 10 where the energies of the various plasma components are displayed as a function of the coupled rf power.

Moreover, if we assume that the power delivered to the electrons has the same dependence on rf power as that shown by p_e in Fig. 9, we conclude that ICRF does not result in a large deterioration of the electron energy transport in PLT for the range of power investigated. In fact, while the value of p_e increases by a factor of ~ 4 (Fig. 9), the total electron energy doubles (Fig. 10). Therefore, the electron energy confinement time, at the worst, decreases by a factor no larger than ~ 2 from the ohmic value. The global power balance is summarized in Table I. Here the quantities τ^* and τ^{**} are the gross plasma energy confinement times without and with the radiation losses taken into account, respectively. We see that the plasma confinement time reaches a certain value when the input rf power becomes comparable to the ohmic power, and does not deteriorate with further rf power increase. This must not be considered a scaling of transport with rf power, because the true meaning of τ^* is only that of a lower limit to the true plasma confinement time. In fact, we do not know whether 100% of the coupled rf power is transferred to the core plasma, or what fraction of the energy of the fast minority ions is lost.

It is noteworthy that while the radiation loss does increase with the application of rf power, the fraction of radiated power is similar to that in ohmic plasmas. Consequently, during rf heating, radiation losses remain a small part of the total power balance.

ACKNOWLEDGMENTS

We gratefully acknowledge the many contributions to this work of the PLT Support Groups and the Engineering Division Staff, and the continued support of Dr. H. Furth, Dr. D. Meade, and Dr. P. Rutherford.

This work supported by US Department of Energy Contract No. DE-AC02-76-CHO-3073.

REFERENCES

[1] HOSEA, J.C., et al., in Proc. of the 8th Int. Conf. on Plasma Physics and Controlled Nuclear Fusion Research, Brussels, Belgium, 1980 (IAEA, Vienna, 1981), Vol. II, p. 95.

[2] HWANG, D., et al., in Proc. of the 9th Int. Conf. on Plasma Physics and Controlled Nuclear Fusion Research, Baltimore, 1982 (IAEA, Vienna, 1983) Vol. II, p. 3.

[3] HWANG, D., et al., J. Vac. Sci. Technol. 20 4 (1981) 1273.

[4] HOSEA, J.C., et al., in Proc. of the 4th Int. Symposium on Heating in Toroidal Plasmas, Rome, Italy, 1984 (ENEA, Rome, 1984), Vol. I, p. 261.

[5] COHEN, S.A., et al., Nucl. Fusion (to be published).

[6] HOSEA, J.C., et al., Phys. Rev. Lett. 43 (1979) 1802.

TABLE I

P_{OH} (MW)	0.7	~ 0.7	~ 0.7	~ 0.7
P_{rf} (MW)	0	0.9	1.9	2.6
P_{rad} (MW)	0.25	0.55	0.75	0.9
E_{tot} (kJ)	24	39	55	69
τ *(msec)	34	24	21	21
τ**(msec)	53	37	30	29

FIGURE CAPTIONS

FIG. 1 Line average electron density (dotted line) and total radiated power as a function of time for P_{rf} = 2.6 MW.

FIG. 2 Time evolution of the central ion temperature derived from: charge exchange (squares), Doppler broadening of the FeXXV line (circles), neutron emission (triangles) for P_{rf} = 2.6 MW and $n_e(o) = 5 \times 10^{13}$ cm^{-3}.

FIG. 3 Time evolution of impurities for P_{rf} = 2.6 MW and $\bar{n}_e = 3.8 \times 10^{13}$ cm^{-3}.

FIG. 4 Radial profiles of ion temperature from Doppler broadening of impurity lines for $\bar{n}_e = 3.8 \times 10^{13}$ cm^{-3}.

FIG. 5 Central ion temperature increase as a function of rf power for $\bar{n}_e$ = $3.6 \times 10^{13} cm^{-3}$ (top) and as a function of $\bar{n}_e$ for P_{rf} = 1 MW (bottom).

FIG. 6 Time evolution of T_e derived from second harmonic electron cyclotron emission at different radial locations for P_{rf} = 2.6 MW and $\bar{n}_e$ = 3.8 $\times 10^{13} cm^{-3}$.

FIG. 7 Electron temperature profiles from Thomson scattering for P_{rf} = 2.6 MW. Top: at the top of a sawtooth oscillation. Bottom: at 1 msec after the internal relaxation.

FIG. 8 Time evolution of $T_e(o)$ during a sawtooth oscillation; A-ohmic, B-0.9 MW, C-2.6 MW.

FIG. 9 Values of $p_e = 1.5\ n_e(o) dT_e(o)/dt$ as a function of rf power (top) and as a function of $\eta = n_{^3He}/n_e$ for $P_{rf} = 1.8$ MW (bottom).

FIG. 10 Energy of plasma components as a function of rf power (^{3}He energy from quasilinear theory).

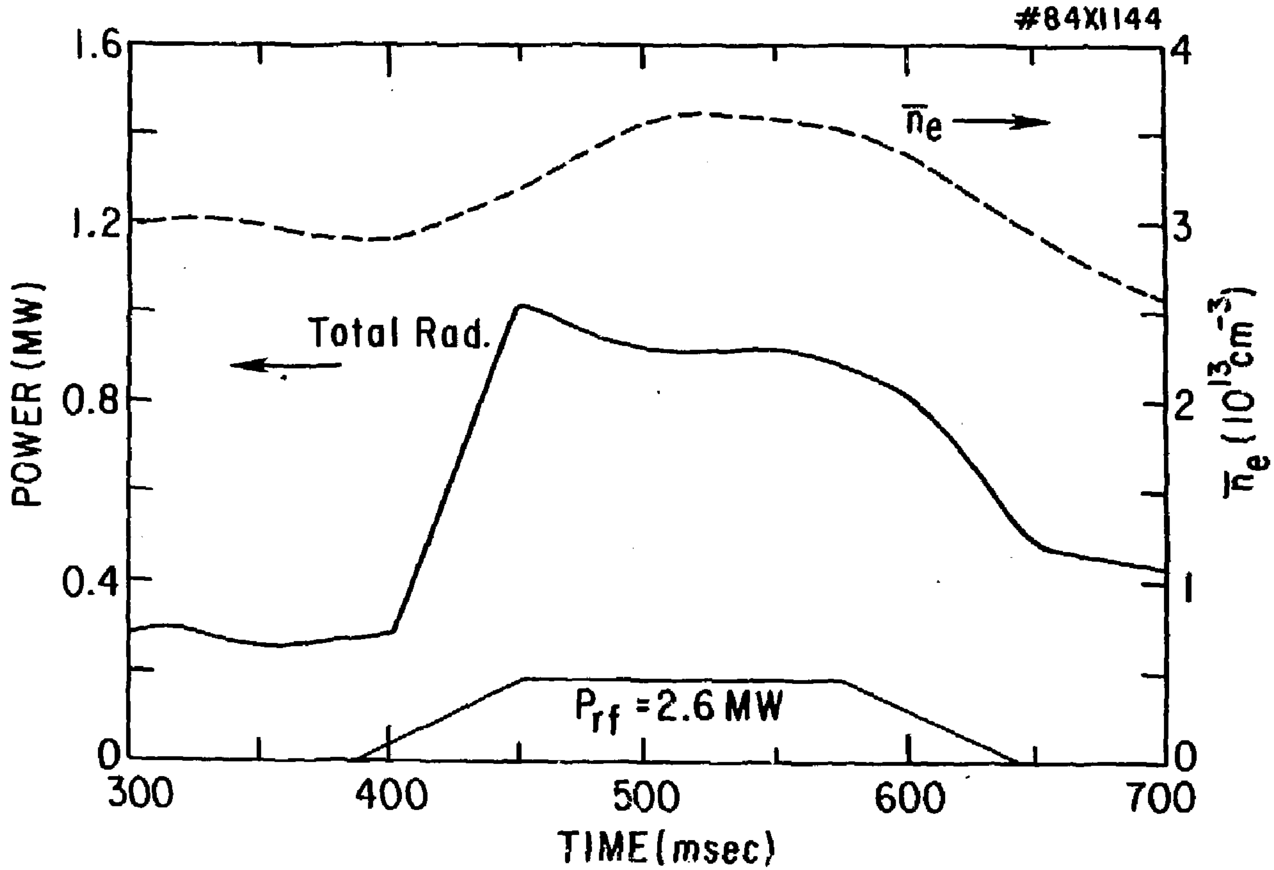
#84X1144
1.6
1.2
0.8
0.4
0
4
3
2
1
0
300
400
500
600
700
TIME (msec)
POWER (MW)
$\bar{n}_e$ (10^{13}cm^{-3})
$\bar{n}_e$
Total Rad.
P_{rf} = 2.6 MW

Fig. 1

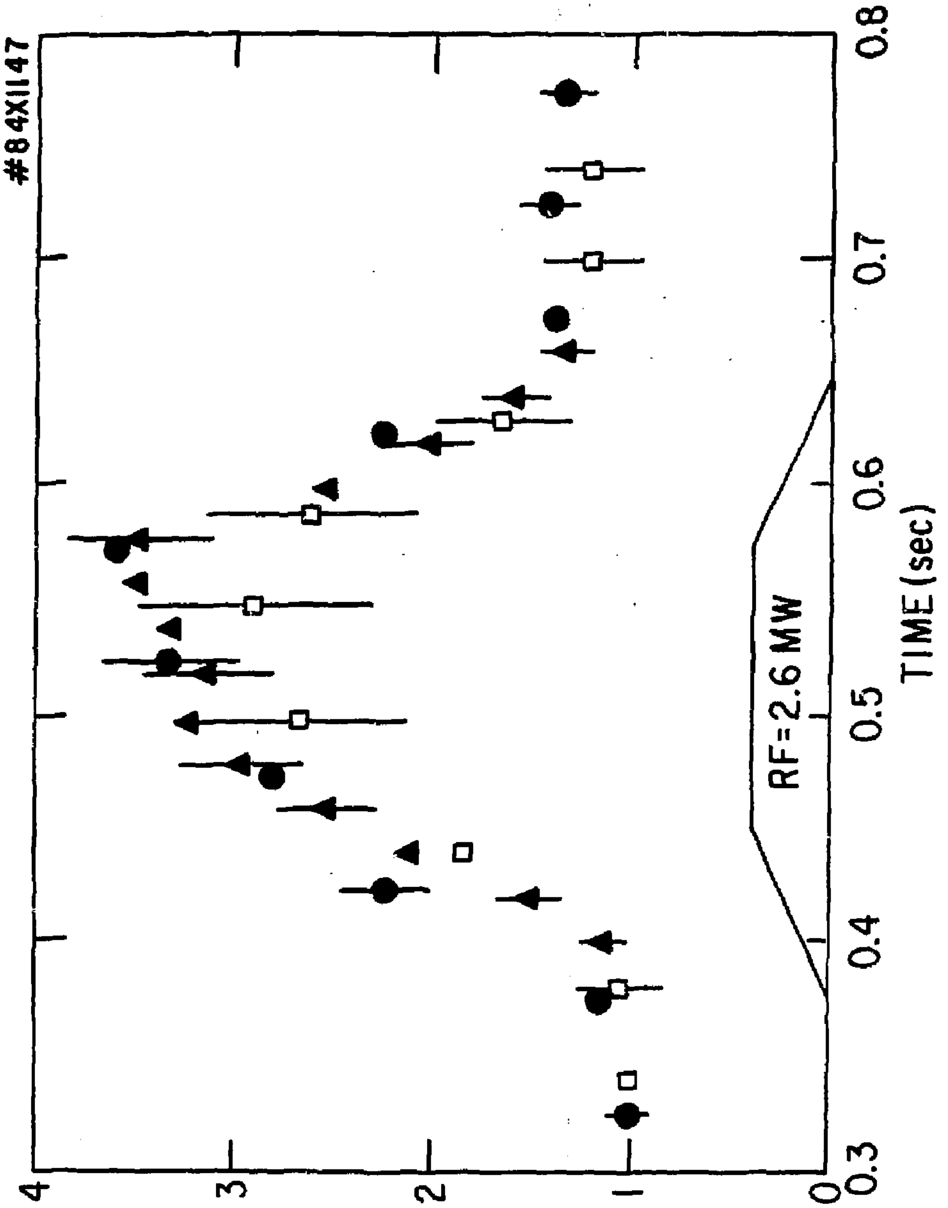

Fig. 2

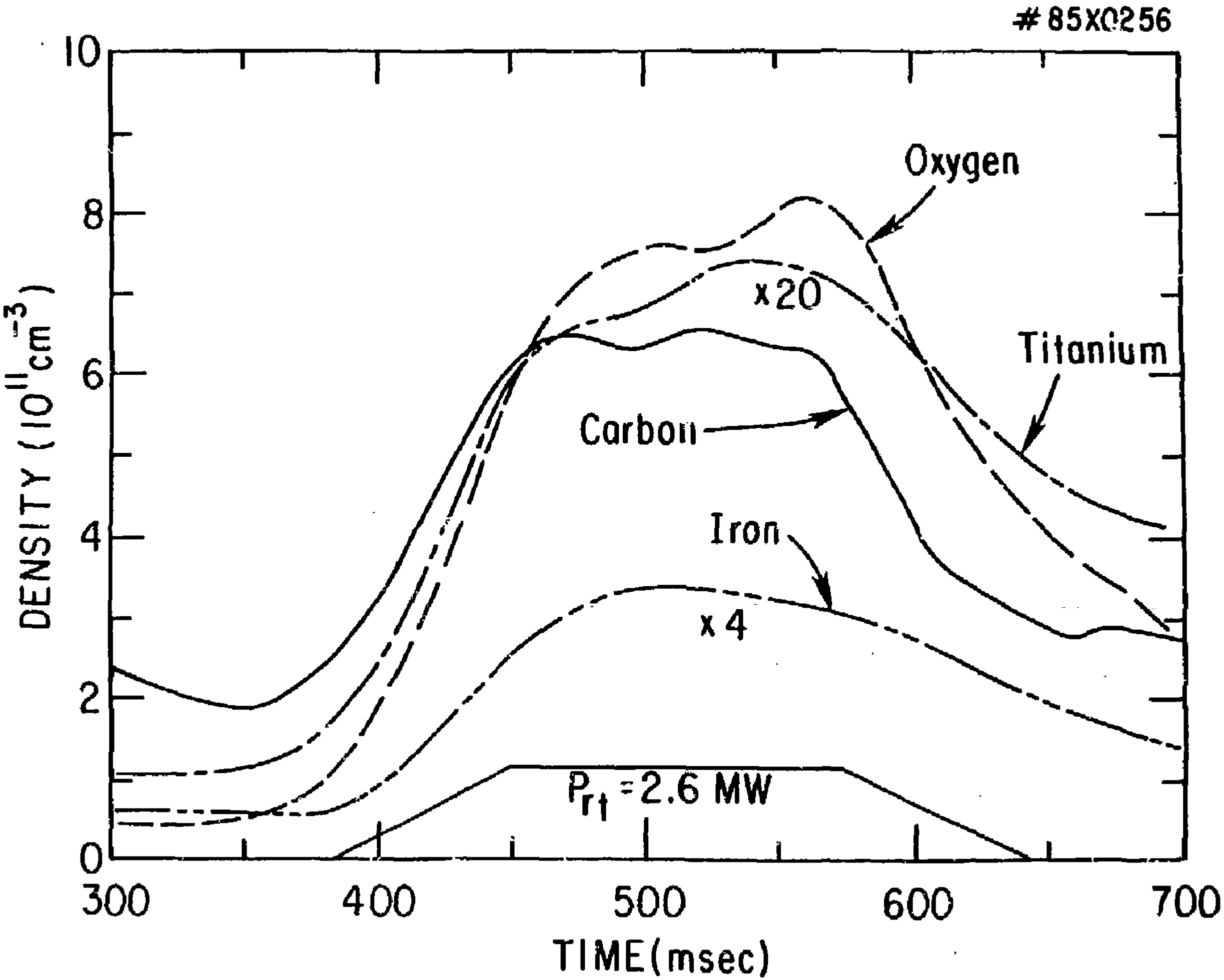
#85X0256
DENSITY (10^{11} cm^{-3})
TIME(msec)
Oxygen
x20
Titanium
Carbon
Iron
x 4
P_{rf} = 2.6 MW
0
2
4
6
8
10
300
400
500
600
700

Fig. 3

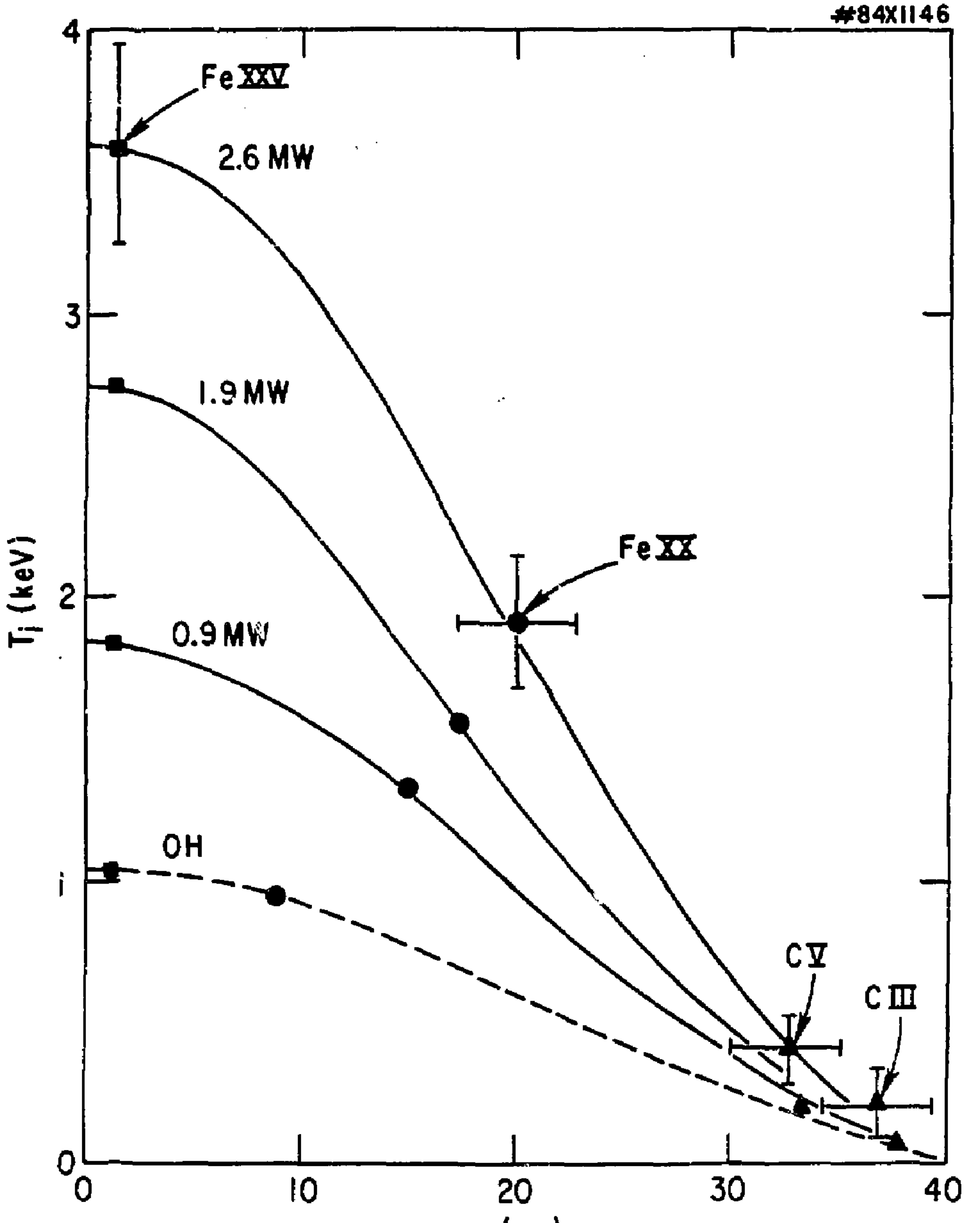
#84X1146
Fe XXV
2.6 MW
1.9 MW
0.9 MW
OH
Fe XX
C V
C III
T_i (keV)
r (cm)
0
1
2
3
4
0
10
20
30
40

Fig. 4

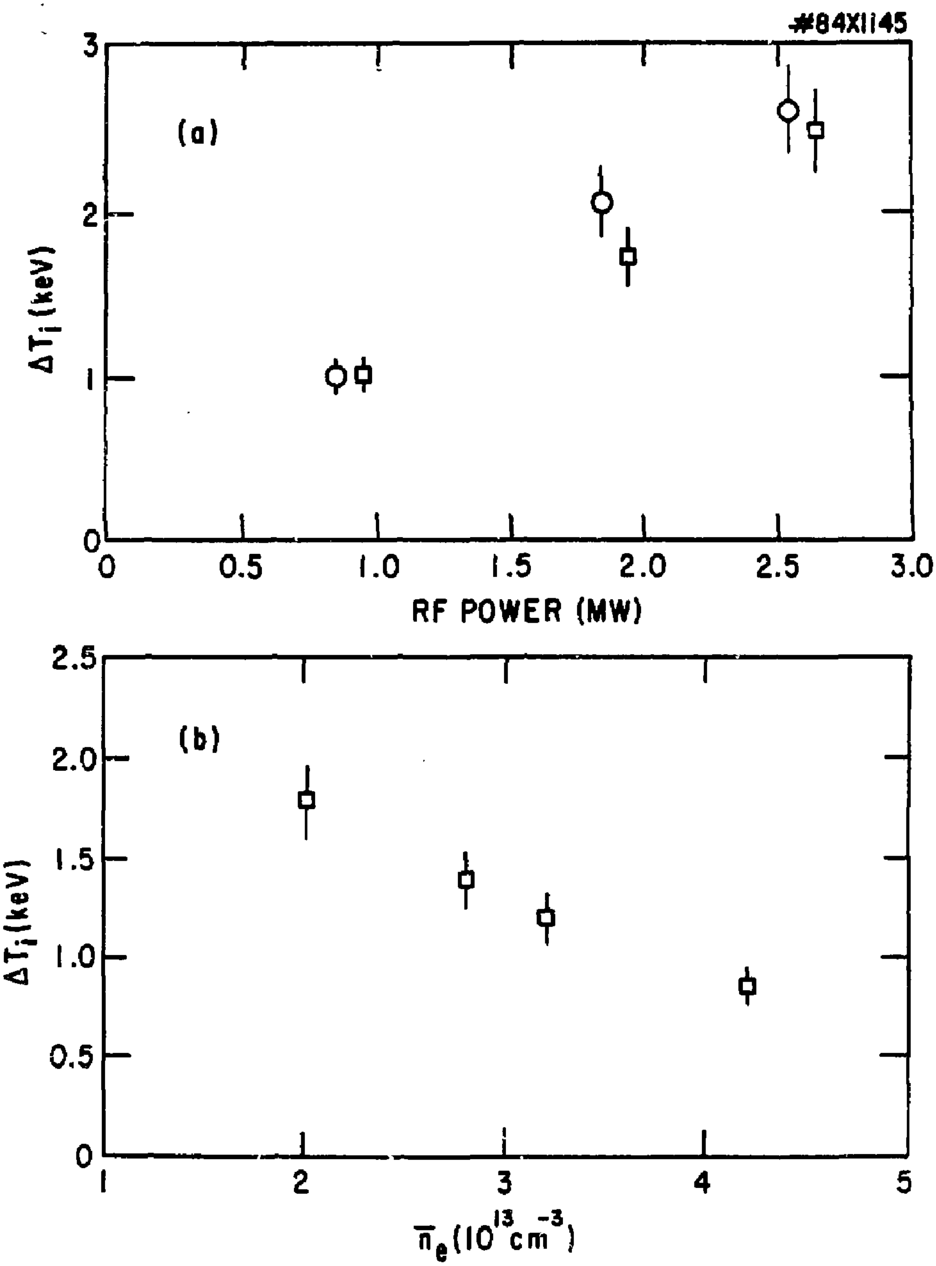
#84X1145
(a)
ΔT_i (keV)
3
2
1
0
0
0.5
1.0
1.5
2.0
2.5
3.0
RF POWER (MW)
(b)
ΔT_i (keV)
2.5
2.0
1.5
1.0
0.5
0
1
2
3
4
5
n̄_e (10^13 cm^-3)

Fig. 5

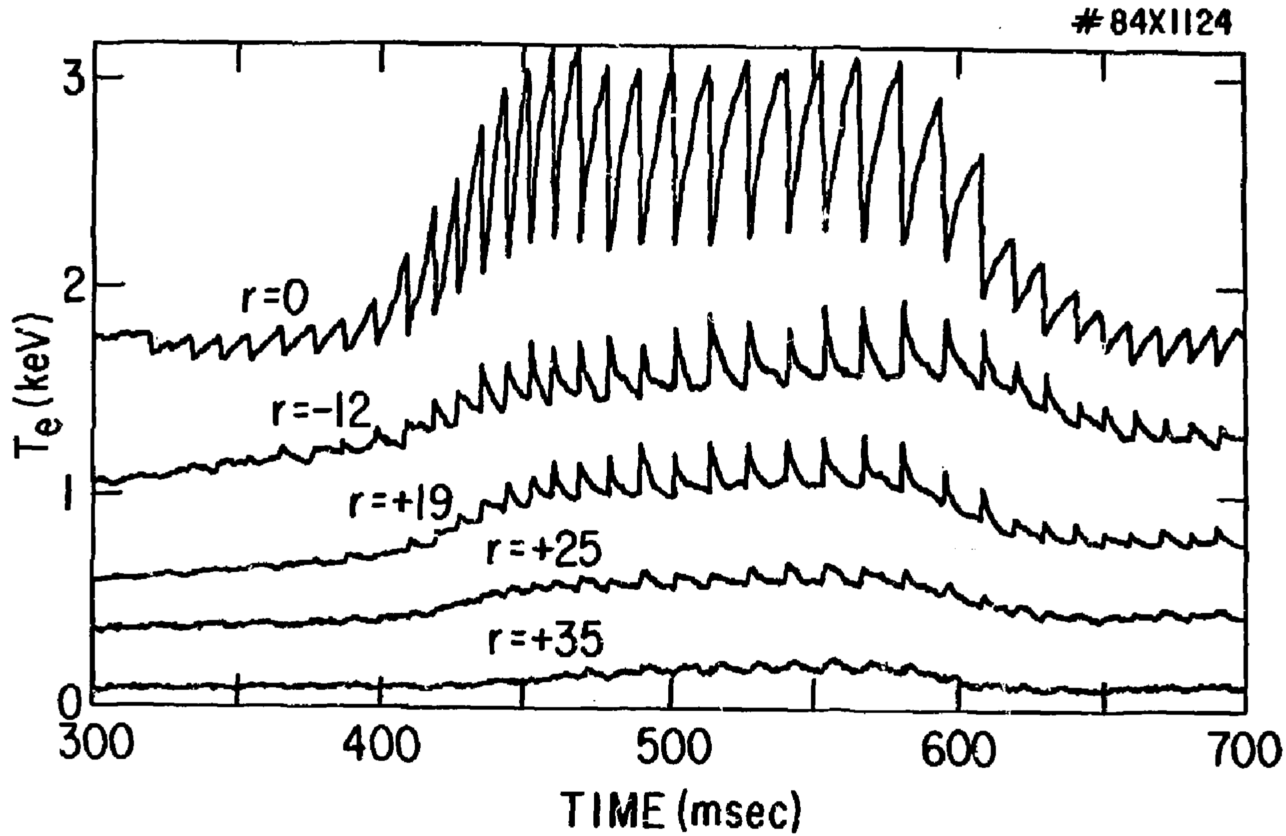
#84X1124
3
2
1
0
T_e (keV)
r=0
r=-12
r=+19
r=+25
r=+35
300
400
500
600
700
TIME (msec)

Fig. 6

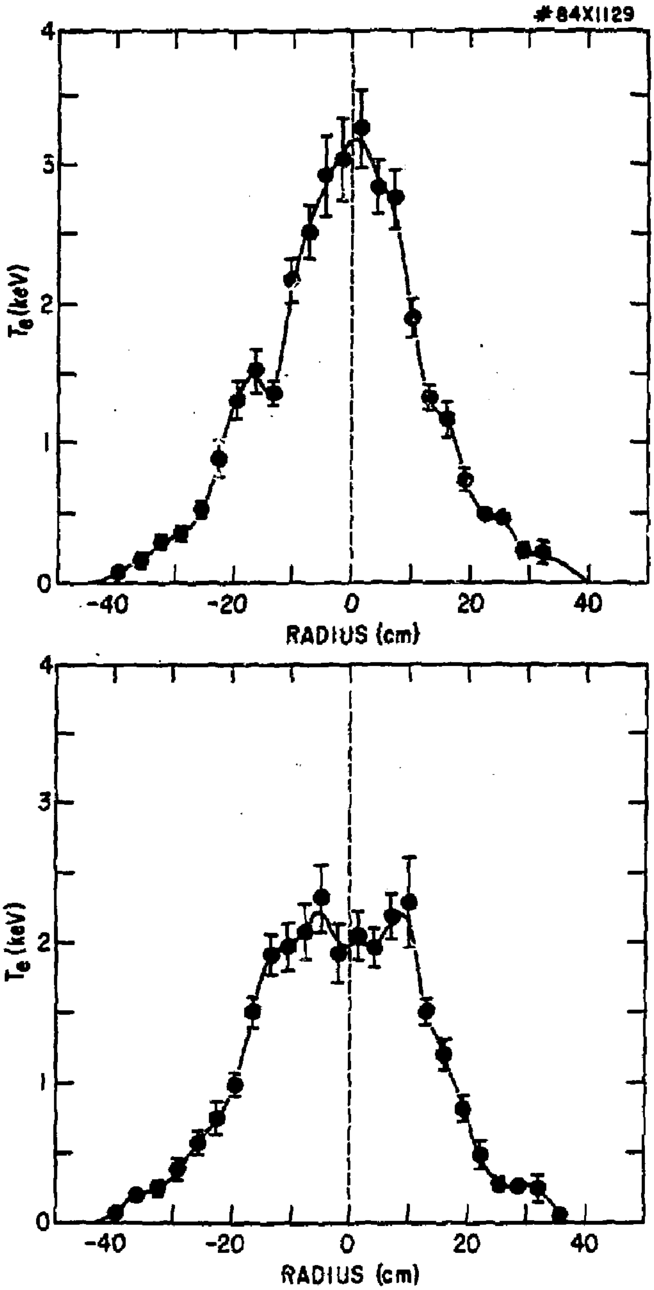

Fig. 7

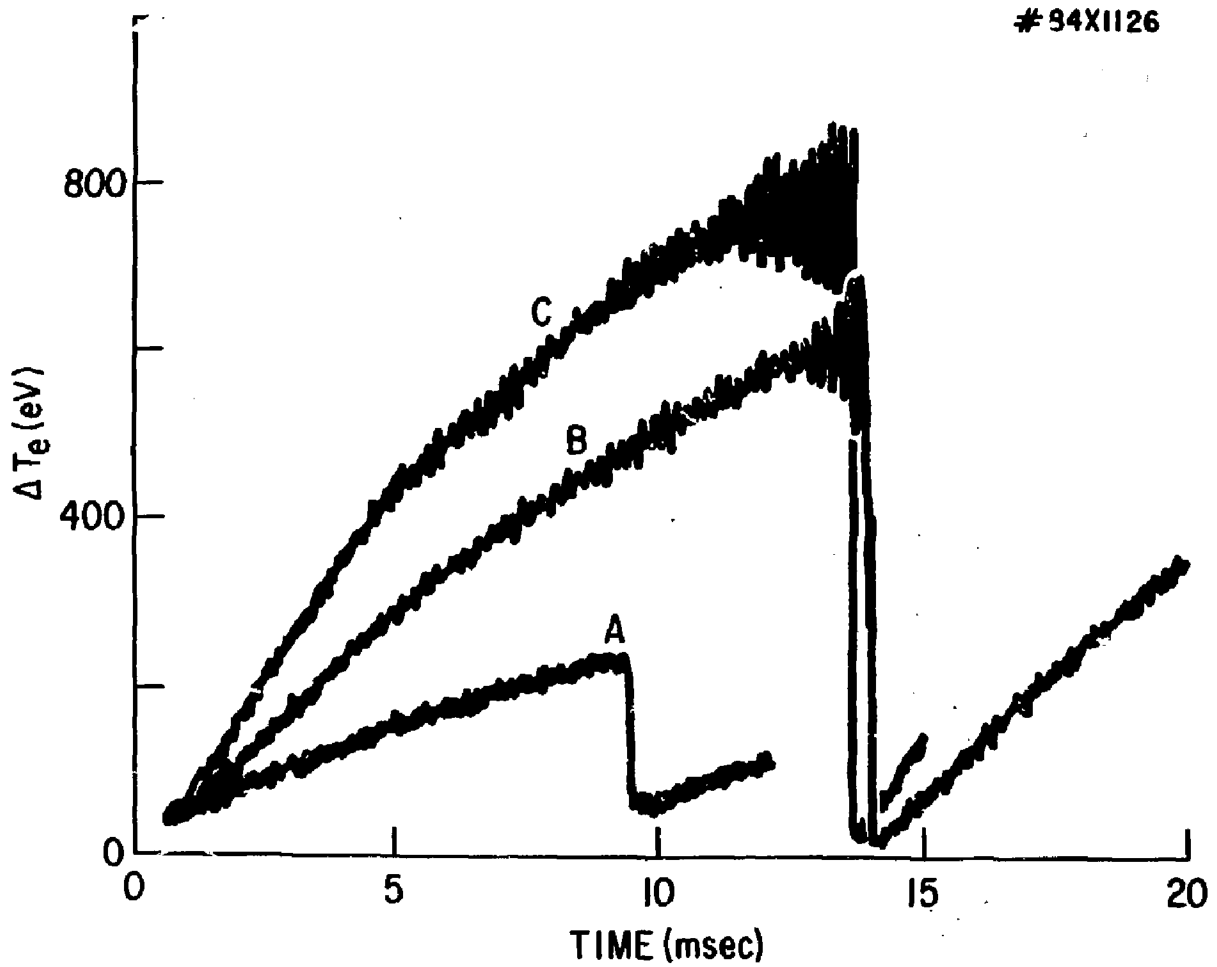

Fig. 8

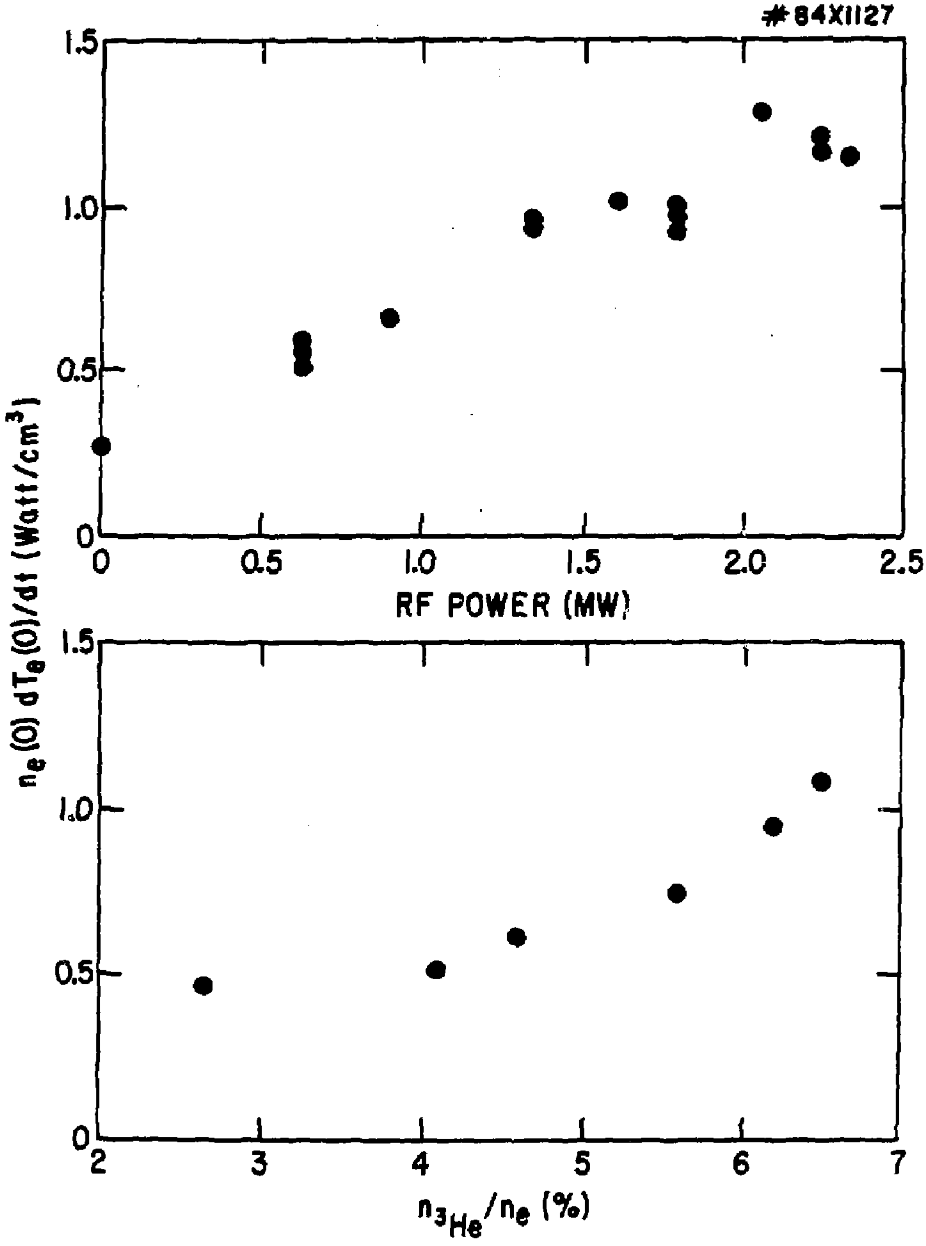

#84X1127
1.5
1.0
0.5
0
0
0.5
1.0
1.5
2.0
2.5
RF POWER (MW)
$n_e(0)\, dT_e(0)/dt$ (Watt/cm^3)
1.5
1.0
0.5
0
2
3
4
5
6
7
$n_{^3He}/n_e$ (%)

Fig. 9

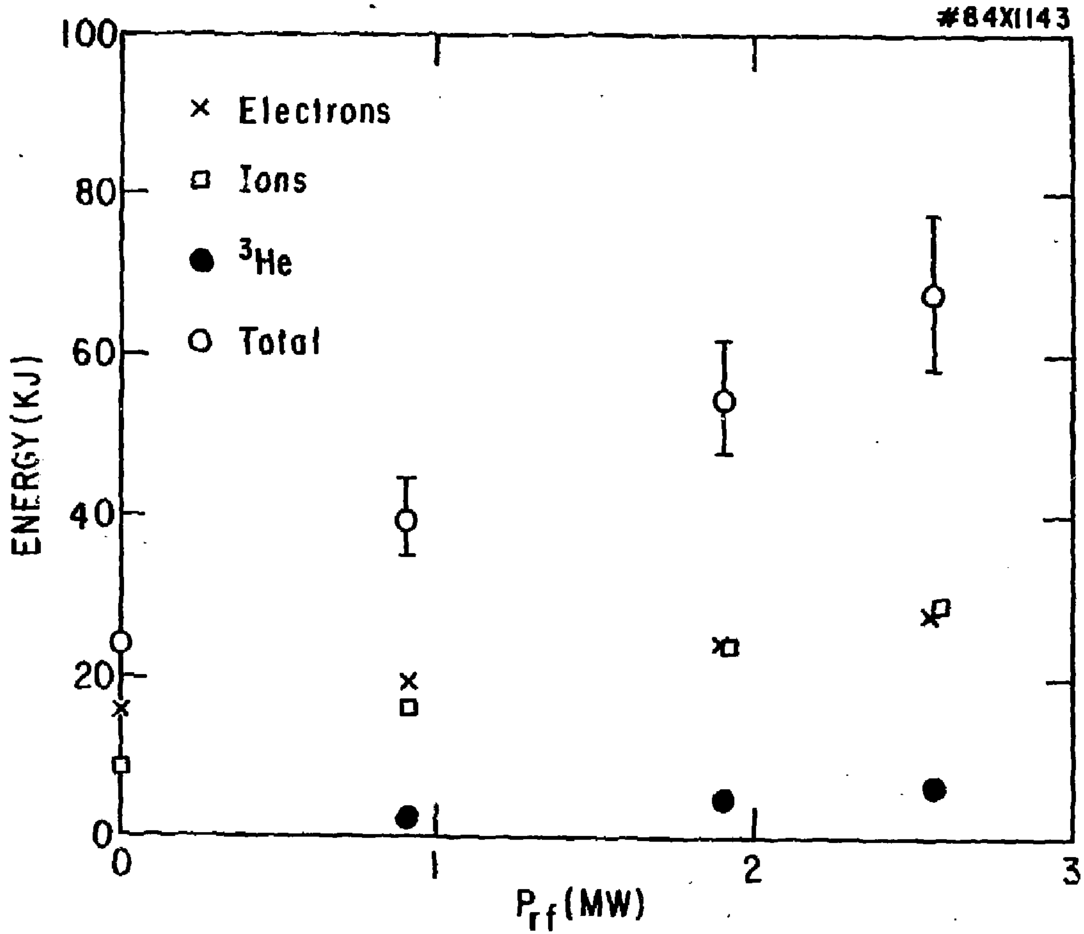
#84X1143
× Electrons
□ Ions
● ³He
○ Total
ENERGY (KJ)
0
20
40
60
80
100
0
1
2
3
P_{rf} (MW)

Fig. 10

EXTERNAL DISTRIBUTION IN ADDITION TO UC-20

Plasma Res Lab, Austra Nat'l Univ, AUSTRALIA
Dr. Frank J. Paoloni, Univ of Wollongong, AUSTRALIA
Prof. I.R. Jones, Flinders Univ., AUSTRALIA
Prof. M.H. Brennan, Univ Sydney, AUSTRALIA
Prof. F. Cap, Inst Theo Phys, AUSTRIA
Prof. Frank Verheest, Inst theoretische, BELGIUM
Dr. D. Palumbo, Dg XII Fusion Prog, BELGIUM
Ecole Royale Militaire, Lab de Phys Plasmas, BELGIUM
Dr. P.H. Sakanaka, Univ Estadual, BRAZIL
Dr. C.R. James, Univ of Alberta, CANADA
Prof. J. Teichmann, Univ of Montreal, CANADA
Dr. H.M. Skarsgard, Univ of Saskatchewan, CANADA
Prof. S.R. Sreenivasan, University of Calgary, CANADA
Prof. Tudor W. Johnston, INRS-Energie, CANADA
Dr. Hannes Barnard, Univ British Columbia, CANADA
Dr. M.P. Bachynski, MPB Technologies, Inc., CANADA
Chalk River, Nucl Lab, CANADA
Zhengwu Li, SW Inst Physics, CHINA
Library, Tsing Hua University, CHINA
Librarian, Institute of Physics, CHINA
Inst Plasma Phys, Academia Sinica, CHINA
Dr. Peter Lukac, Komenskeho Univ, CZECHOSLOVAKIA
The Librarian, Culham Laboratory, ENGLAND
Prof. Schatzman, Observatoire de Nice, FRANCE
J. Radet, CEN-BP6, FRANCE
AM Dupas Library, AM Dupas Library, FRANCE
Dr. Tom Mual, Academy Bibliographic, HONG KONG
Preprint Library, Cent Res Inst Phys, HUNGARY
Dr. S.K. Trehan, Panjab University, INDIA
Dr. Indra Mohan Lal Das, Banaras Hindu Univ, INDIA
Dr. L.K. Chavda, South Gujarat Univ, INDIA
Dr. R.K. Chhajlani, Vikram Univ. INDIA
Dr. B. Dasgupta, Saha Inst, INDIA
Dr. P. Kaw, Physical Research Lab, INDIA
Dr. Phillip Rosenau, Israel Inst Tech, ISRAEL
Prof. S. Cuperman, Tel Aviv University, ISRAEL
Prof. G. Rostagni, Univ Di Padova, ITALY
Librarian, Int'l Ctr Theo Phys, ITALY
Miss Clelia De Palo, Assoc EURATOM-ENEA, ITALY
Biblioteca, del CNR EURATOM, ITALY
Dr. H. Yamato, Toshiba Res & Dev, JAPAN
Direc. Dept. Lg. Tokamak Dev. JAERI, JAPAN
Prof. Nobuyuki Inoue, University of Tokyo, JAPAN
Research Info Center, Nagoya University, JAPAN
Prof. Kyoji Nishikawa, Univ of Hiroshima, JAPAN
Prof. Sigeru Mori, JAERI, JAPAN
Library, Kyoto University, JAPAN
Prof. Ichiro Kawakami, Nihon Univ, JAPAN
Prof. Satoshi Itoh, Kyushu University, JAPAN
Dr. D.I. Choi, Adv. Inst Sci & Tech, KOREA
Tech Info Division, KAERI, KOREA
Bibliotheek, Fom-Inst Voor Plasma, NETHERLANDS
Prof. B.S. Liley, University of Waikato, NEW ZEALAND
Prof. J.A.C. Cabral, Inst Superior Tecn, PORTUGAL
Dr. Octavian Petrus, ALI CUZA University, ROMANIA
Prof. M.A. Hellberg, University of Natal, SO AFRICA
Dr. Johan de Villiers, Plasma Physics, Nucor, SO AFRICA
Fusion Div. Library, JEN, SPAIN
Prof. Hans Wilhelmson, Chalmers Univ Tech, SWEDEN
Dr. Lennart Stenflo, University of UMEA, SWEDEN
Library, Royal Inst Tech, SWEDEN
Centre de Recherchesen, Ecole Polytech Fed, SWITZERLAND
Dr. V.T. Tolok, Kharkov Phys Tech Ins, USSR
Dr. D.D. Ryutov, Siberian Acad Sci, USSR
Dr. G.A. Eliseev, Kurchatov Institute, USSR
Dr. V.A. Glukhikh, Inst Electro-Physical, USSR
Institute Gen. Physics, USSR
Prof. T.J.M. Boyd, Univ College N Wales, WALES
Dr. K. Schindler, Ruhr Universitat, W. GERMANY
Nuclear Res Estab, Julich Ltd, W. GERMANY
Librarian, Max-Planck Institut, W. GERMANY
Bibliothek, Inst Plasmaforschung, W. GERMANY
Prof. R.K. Janev, Inst Phys, YUGOSLAVIA